CURRENT STATUS OF INSERTION DEVICE DEVELOPMENT AT THE NSLS-II AND ITS FUTURE PLANS

T. Tanabe, O. Chubar, T. Corwin, D. A. Harder, P. He, C. Kitegi, J. Rank, C. Rhein, G. Rakowsky and C. Spataro
Photon Science Directorate, BNL, Upton, NY 11973, U.S.A.

Abstract

National Synchrotron Light Source-II (NSLS-II) project is currently under construction. Procurement of various insertion devices (IDs) has begun. This ring assumes a very high beam stability requirement which imposes tighter field specifications on insertion devices (IDs) compared to the rings of previous generation. The state of the art ID Magnetic Measurement Facility is being set up in order to be able to certify the stringent requirements on the magnetic field of NSLS-II IDs. The IDs in the project baseline scope include six 3.5m long damping wigglers (DWs) with 100mm period length and 15mm pole gap, two 2.0m Elliptically Polarizing Undulator (EPU) with 49mm period and 11.5mm minimum magnetic gap, two 3.0m long 20mm period and one 1.5m long 21mm period IVU, which the minimum gap of these is 5mm and 5.5mm, respectively. Recently a special device for inelastic X-ray scattering (IXS) beamline has been added to the collection of baseline devices. Three pole wigglers with a 28mm magnetic gap and a peak field over 1 Tesla will be utilized to accommodate the users of the type of radiation which is currently produced with bending magnets at the NSLS.

Introduction

NSLS-II ID parameters have been unchanged since May 2010 [1]. Updates of the baseline devices and related activities are explained below.

DW

A vendor has been chosen for the procurement of the 6 DWs in November 2010. A Preliminary Design Review has been conducted to finalize the magnetic design and preliminary mechanical design. Even though the operating gap of this DW is fixed at 15.0mm, some effort has been made to minimize the change in the field error at bigger gap settings so that the electron beam will not be lost in case of an emergency gap opening. The magnetic structure is NdFeB based hybrid design with side magnets. The support structure is a C-frame and compensation springs are used to reduce the variation of forces on the ball spindle. Figure 1 shows the vendor's 3D-CAD rendering of a DW.

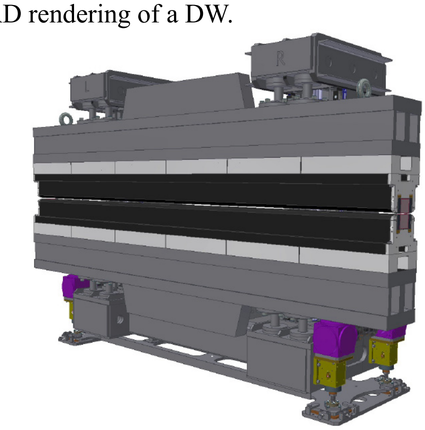

Figure 1: 3D-CAD rendering of NSLS-II DW.

3PW

3PW procurement is in the final stage of signing a contract with the selected vendor. Unlike other devices, BNL design will be used without much modification to preserve the detailed spectral characteristics of the device.

EPU

A vendor has been selected for two 2m long EPUs. The contract will be issued by mid April in 2011. Strong emphasis is made on the force calculations on the mechanical units with various gap / phase combinations to prevent uncontrollable field quality variations. A dynamic compensation scheme using current carrying strips proposed and implemented elsewhere will be employed for non-linear correction [1]. First the optimization was done to compensate the effect of the second order kicks [2] in the mid-plane [3]. However, this compensation scheme to minimize trajectory deviation does not necessary minimize the tune foot print.

We are currently working to improve the compensation by including off-the-midplane points for the current optimization using Radia [4]. Figure 2-A and 2-B show the electron trajectory angles at exit of 2 m long EU49 in vertical linear polarization mode at different initial transverse positions. As is expected, the trajectories in both planes deviate from those optimized for trajectory straightness. (Figure 3-A for horizontal trajectory and Fig. 3-B for vertical one, respectively.) So far we have kept the rotation symmetry with respect to Z-axis of the current distributions. Breaking this symmetry may improve the compensation but at the expense of increasing the required number of the power supplies by a factor of two. Preliminary tracking studies show

Notice: This manuscript has been authored by Brookhaven Science Associates, LLC under Contract No. DE-AC02-98CH1-886 with the U.S. Department of Energy. The United States Government retains, and the publisher, by accepting the article for publication, acknowledges, a world-wide license to publish or reproduce the published form of this manuscript, or allow others to do so, for the United Government purposes.

promising results. These results will be presented elsewhere.

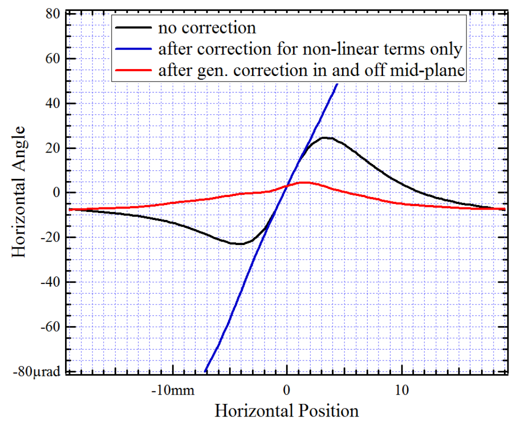

Figure 2-A: Resulting horizontal angle vs horizontal initial position in horizontal mid-plane (at y0 = 0) .

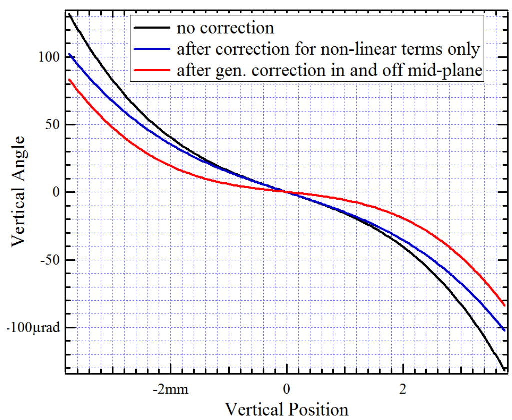

Figure 2-B: Resulting vertical angle vs vertical initial position in vertical mid-plane (at x0 = 0).

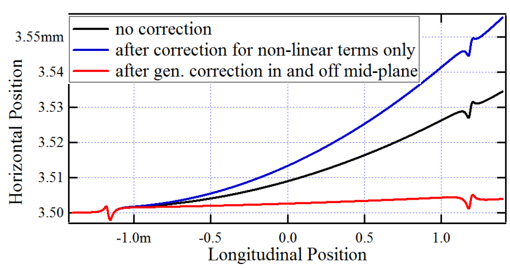

Figure 3-A: Horizontal projections at x0= 3.5 mm, y0= 0 before undulator.

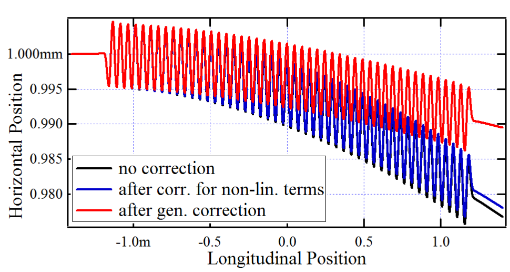

Figure 3-B: Vertical projections at x0= 0, y0= 1 mm before undulator.

IVU

The baseline IVUs are planned to be operated at room temperature. A standard device is 3m long and a canted version will be 1.5m. The device for IXS beamline will be a special device with wider pole than that of a standard device due to much larger horizontal beta function in a long straight section. The device cross section is also smaller than that of a standard IVU. Cryo Permanent Magnet Undulator (CPMU) option with PrFeB magnet [5] will be one of a viable future upgrade options. A preliminary design incorporates cooling circuits which could be utilized for both cooling water and, in the case of CPMU, liquid nitrogen. This design is based on the previously fabricated MGU-X25 [6] and MGU-X9 design. Therefore the principle is proven in at least four working devices at the NSLS. Figure 4 shows the latest jacketed fluid feedthrough design shared with structural feedthrough.

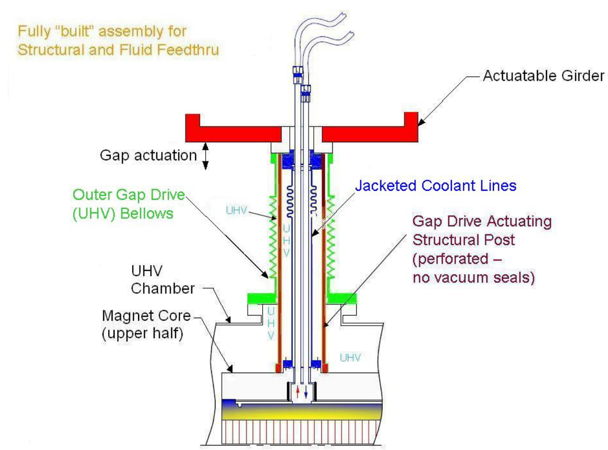

Figure 4: Jacketed fluid feedthrough design shared with structural feedthrough used by four IVUs at the BNL.

The advantages of this design compared to a conventional design using clamped or brazed coolant tube penetrating simple fluid feedthrough are as follows:

- Structural and fluid connections share common feedthrough.
- Lower probability of air-to-UHV leak
- Negligible probability of water-to-UHV leak
- Cooling channel leak is to ambient room only and may usually be repaired without breaking vacuum.
- No fatigue stress induced in thin wall tubing.
- Allows for magnet array upgrade to CPMU (Jacket can accommodate vacuum insulation) with negligible increase in cost.

Figure 5 delineates our multiple metered cooling circuit design which has the advantage of better control of cooling flow distribution to non-uniform heat load. Comparison of temperature distribution is made between standard design approach and BNL's design. The heat load distribution used in the simulation is shown in Fig. 6 and the resulting temperature distributions are shown in

Fig. 7. Our goal is to keep the longitudinal temperature gradient less than 0.5 K/m to avoid deterioration of spectral characteristic.

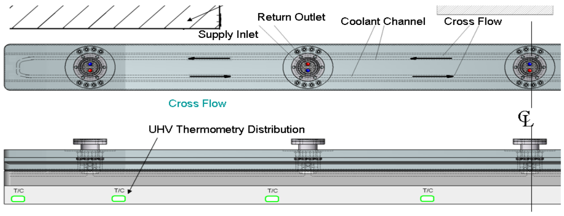

Figure 5: Coolant Cross-Flow Distribution Manifold.

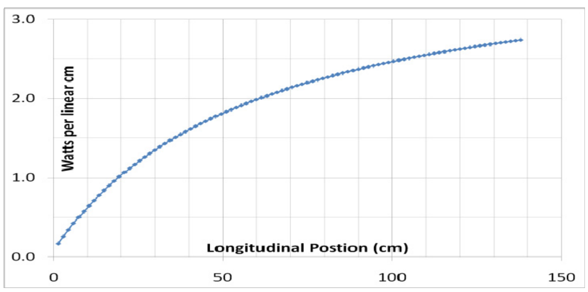

Figure 6: Heat load distribution applied in the simulation in addition to 5W end load due to flex transition.

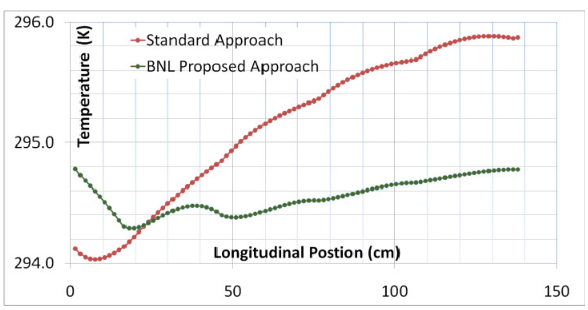

Figure 7: Comparison of magnet temperature variation along beam axis for "standard" vs. proposed approach.

ID-MMF

To further improve the accuracy and repeatability of our Hall probe data we have made some upgrades to our Hall probes and the related data acquisition electronics. We use the National Instruments Compact RIO real-time Programmable Automation Controller, which integrates a Field Programmable Gate Array on the backplane with a dedicated real-time processor. VHDL compiler renders the user programs in FPGA executable bit files. Thus it is possible to imbed timing and DAQ features associated with on-the-fly Hall bench data acquisition on the FPGA, and manipulate the features of the digital and analog modules directly from the FPGA.

Using this venue, we intend to implement a new probe which has a 24 bit sigma-delta analog to digital convertor IC at the probe, close to the Hall elements. The ADC is a low power device which can be battery powered. It has three input channels, a low-noise programmable-gain instrumentation amp, a pair of constant current sources, a precision band-gap reference, and a 64 kHz modulator clock on-chip—it is a complete low-noise ADC subsystem in tiny 16-lead surface-mount chip. The chip can be interfaced with the Compact RIO via a digital IO module, and so the SPI interface can be implemented at the FPGA level. The on-the-fly data capture signal is provided by the linear encoder signal from the Kugler Hall bench (shown in Fig. 8 below) Z-axis, via the Delta Tau motion controller. That trigger signal is fed into the FPGA, which makes it possible to precisely synchronize the data capture positions, and achieve high spatial repeatability in the measurements, and the real-time processor can build arrays of Hall voltage samples, perform floating –point computations to remove offset, to apply compensation for temp variation and for planar Hall, and to apply polynomial interpolation to convert Hall probe voltage to B field.

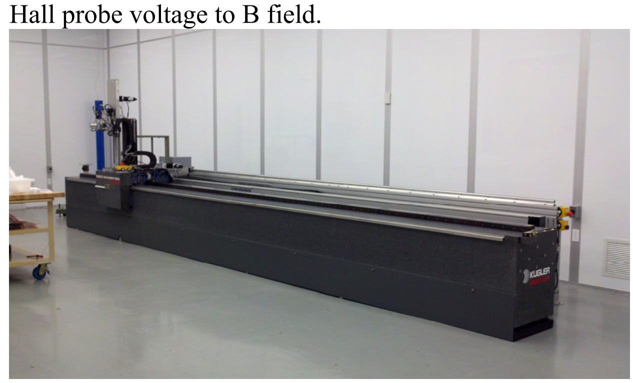

Figure 8: 6.5m Hall probe bench built by Kugler, GmbH.

FUTURE DEVICES

R&D activities are conducted to create bakable PrFeB based CPMU. Prototype models are being fabricated and the final device i will be 2.7m long with a 17mm period..

A super conducting wiggler (SCW) is planned to be installed in one of the short straights in the NSLS-II ring. The current (tentative specification) is a 1m device with 80mm period and 4.5T maximum field.

REFERENCES

[1] J. Bahrdt, *et. al.,* "Active shimming of the dynamic multipoles of the BESSY UE112 Apple Undulator", Proceedings of EPAC'08, p. 2222 (2008).
[2] P. Elleaume, "A New Approach to the Electron Beam Dynamics in Undulators and Wigglers.", Proceedings of EPAC92, p. 661 (1992).
[3] T. Tanabe, *et. al.*, "Progress On Insertion Device Related Activities At The NSLS-II And Its Future Plans.", Proceedings of IPAC10, p3204 (2010).
[4] O. Chubar, P. Elleaume, and J. Chavanne, J. Synchrotron Rad. 5, pp.481 - 484 (1998).
[5] T. Tanabe, *et. al.*, "Cryo-temperature field measurement of PrFeB undulator and performance enhancement options at the NSLS-II," Proceedings of SRI09, p.29 (2010).
[6] T. Tanabe, *et. al.*, "X-25 cryo-ready in-vacuum undulator at the NSLS," AIP Conference Proceedings Volume 879, pp283, (2006).